Addressing Multiple Nodes in Networked Labs-on-Chips without Payload Re-injection

Werner Haselmayr*, Andrea Biral‡, Andreas Grimmer†, Andrea Zanella‡, Andreas Springer*, Robert Wille†
*Institute for Communications Engineering and RF-Systems, Johannes Kepler University Linz, Austria
†Institute for Integrated Circuits, Johannes Kepler University Linz, Austria
{werner.haselmayr, andreas.grimmer, andreas.springer, robert.wille}@jku.at
‡Department of Information Engineering, University of Padova, Italy
{biraland, zanella}@dei.unipd.it

***Abstract*—On a droplet-based *Labs-on-Chip* (LoC) device, tiny volumes of fluids, so-called droplets, are flowing in channels of micrometer scale. The droplets contain chemical/biological samples that are processed by different modules on the LoC. In current solutions, an LoC is a single-purpose device that is designed for a specific application, which limits its flexibility. In order to realize a multi-purpose system, different modules are interconnected in a microfluidic network – yielding so-called *Networked LoCs* (NLoCs). In NLoCs, the droplets are routed to the desired modules by exploiting hydrodynamic forces. A well established topology for NLoCs are ring networks. However, the addressing schemes provided so far in the literature only allow to address multiple modules by re-injecting the droplet at the source every time, which is a very complex task and increases the risk of ruining the sample. In this work, we address this issue by revising the design of the network nodes, which include the modules. A novel configuration allows that the droplet can undergo processing several times in cascade by different modules with a single injection. Simulating the trajectory of the droplets across the network confirmed the validity of our approach.**

***Index Terms*—Droplet-based microfluidics, labs-on-chip, networked labs-on-chip, passive switching and sorting**

I. Introduction

Labs-on-Chips (LoCs) allow for the miniaturization, integration and automation of chemical and biomedical procedures [1]. They integrate different laboratory functions on a single chip and are successfully employed e.g. for DNA sequencing, cell analysis, organism analysis or drug screening [2]. Droplet-based microfluidic systems [3] are a promising platform for the realization of LoCs. In droplet-based microfluidics, tiny volumes of fluids, so-called droplets, are controlled and manipulated. This is achieved by means of two different approaches: The *surface-based approach* allows to arbitrarily move droplets on a planar (open) surface by electrowetting-on-dielectric [4] or by surface acoustic waves [5]. This offers high flexibility because the path of the droplet is freely programmable. However, surface-based approaches suffer from the evaporation of liquids, the fast degradation of the surface coatings, its lacking biocompatibility and the complex and costly fabrication process [2]. In *channel-based approaches* (see e.g., [3]), the droplets flow in closed microchannels, triggered by some external force (e.g., pressure pump) at the chip boundary. The closed channels allow for an incubation and storage of liquid assays over a long period of time and, hence, avoid evaporation and unwanted reactions [2]. However, the channel-based approach lacks in flexibility since current LoC solutions are designed for a specific application. To overcome this issue, networking and communication capabilities were added to LoCs [6] – yielding so-called *Networked LoCs* (NLoCs). In NLoCs, the droplets are passively routed in the channel by exploiting hydrodynamic forces that are mainly determined by the channel geometry only. Thus, NLoCs are a promising solution for the realization of flexible and biocompatible LoCs that can be fabricated at low cost (e.g., using 3D printers).

A. Review of NLoCs

The idea of NLoCs was, for the first time, introduced in [6]. Currently, there are two well established topologies for NLoCs: Ring [6], [7] and bus [8], [9] networks. In such networks, so-called *payload* droplets, including chemical or biological samples, are sent to the network nodes for processing. The addressing of the network nodes is accomplished through sending a so-called *header* droplet in front of the payload droplet. Header droplets are only used for signaling and contain no samples. The address can be either encoded in the distance between the payload and the header droplet [6] or in the size of the header droplet [8]. Although, currently, only ring and bus networks are considered, the addressing scheme employing header droplets is also applicable for other network topologies.

A major drawback of the aforementioned addressing scheme is that a payload droplet can only be sent to a single network node at a time. If the payload droplet needs to be processed by multiple nodes, it is re-injected at the source after each processing step and a new header droplet is generated for addressing the next node. The re-injection of droplets into the system is a complex task and increases the risk of ruining the sample. Thus, this approach is not practical, especially, when the payload droplets has to be processed by several nodes.

B. Contribution

The aim of this work is to enable NLoC systems to address multiple nodes with a single injection. The proposed scheme should especially consider scenarios where a droplet has to be processed by many nodes. To this end, we are making the following contributions:

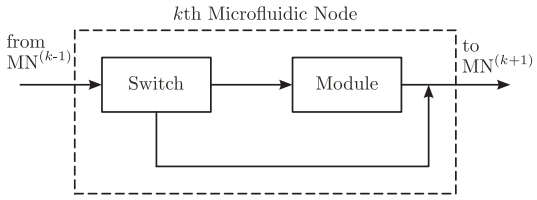

Fig. 1. State-of-the-art microfluidic node (MN$^{(k)}$ is the kth microfludic node).

- We revise the network node by introducing new blocks, namely a sorter and a delay line.
- We show that the proposed solution is especially suited when the payload droplet has to be processed by many nodes (e.g., only one header droplet is required to process the payload droplet by all nodes except one).
- We validate our approach by evaluating the *macroscopic* evolution of the droplets path in the network. This is accomplished by applying the simulator presented in [10].

II. State-of-the-Art Addressing Scheme

In this section, we review, for the sake of completeness, the addressing scheme for the well established ring network [6], [7]. We consider a ring network with K microfluidic nodes. Each node (cf. Fig. 1) includes a microfluidic switch and a microfluidc module. The module performs chemical or biological operations on the payload droplet and the switch, together with the header droplet, decides whether the operation is executed on the payload droplet or not. The switch and its electrical equivalent circuit are shown in Fig. 2[1] . It consists of a T-junction, two asymmetric rectangular channels 1 and 2 and a bypass channel. The hydrodynamic resistance for a rectangular channel with length L, width w and height h is given by [7], [10]

$$R = \frac{\alpha \mu L}{w h^3}, \tag{1}$$

where μ denotes the dynamic viscosity of the carrier fluid. The dimensionless parameter α can be expressed as

$$\alpha = 12 \left[1 - \frac{192h}{\pi^5 w} \tanh\left(\frac{\pi w}{2h}\right) \right]^{-1}. \tag{2}$$

We assume that channel 2 is shorter than channel 1, i.e. $L_2 < L_1$ and, thus, channel 2 has a lower hydrodynamic resistance than channel 1, i.e. $R_2 < R_1$. Due to the bypass channel, the behavior of the switch depends only on the geometry of channel 1 and 2 [7]. The switch is based on the principle that a droplet arriving at the T-junction flows into the channel with the lower hydrodynamic resistance.

The address is encoded in the distance between the payload and the header droplet. Let's consider a payload and a header droplet with a distance of $D_{\text{HP}}^{(k)}$, arriving at the entrance of the kth node and thus at the T-junction of the switch. Since $R_2 < R_1$, the header droplet flows into channel 2 towards the $(k+1)$th node. Depending on the distance $D_{\text{HP}}^{(k)}$, we can distinguish two cases for the payload droplet [7]:

[1]A good review on this analogy can be found in [11].

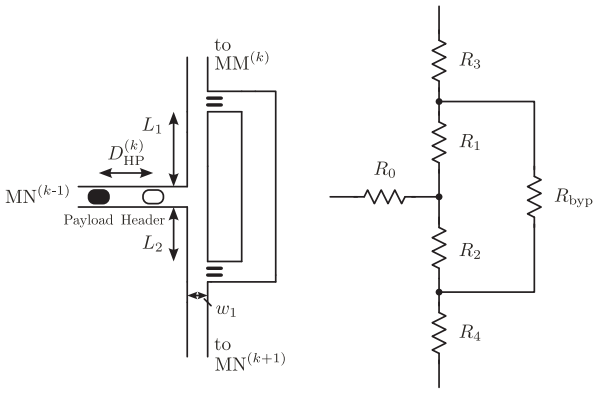

Fig. 2. Distance-based switch [7] and the electrical equivalent circuit (MN$^{(k)}$ denotes the kth microfludic node and MM$^{(k)}$ denotes the microfluidic module in the kth node).

1) *Executing the kth module – $D_{HP}^{(k)} < L_2$:* The header droplet is still in channel 2 and increases the hydrodynamic resistance of channel 2 by R_D[2]. In order that the payload droplet flows into channel 1, we must guarantee that $(R_2 + R_D) > R_1$ holds. In this case, the payload droplet flows into the module (channel 1) for processing and, afterwards, towards the $(k+1)$th node. To avoid that subsequent nodes are addressed unintentionally, it must be ensured that the distance between payload and header droplet at the outlet of the kth node is sufficiently large.
2) *Skipping the kth module – $D_{HP}^{(k)} > L_2$:* Since the header droplet has already left channel 2, the payload follows the header droplet into channel 2 towards the $(k+1)$th node. Hence, the payload droplet is skipping the module.

The distance between the payload and the header droplet can be used to address the desired module in the network, which should process the payload droplet. However, the distance decreases as the droplets traverse through the switches. To process the payload droplet by the kth module the distance at the entrance of the first node must be [7]

$$\beta^{k-1} L_2 < D_{\text{HP}}^{(1)} < \beta^k L_2 \quad \text{for } k > 1, \tag{3}$$

with $\beta = (L_1 + L_2)/L_1$.

However, the addressing scheme described above only allows to send the payload droplet to one particular module for processing. If the payload should be processed by multiple modules, the payload needs to be re-injected at the source and a new header droplet has to be generated for addressing the next module. Since the re-injection of droplets is a complex task, which additionally may ruin the sample, an addressing scheme that allows to reach multiple modules is required.

III. Proposed Addressing Scheme

In this section, we propose a scheme that allows the payload droplet to address multiple modules without re-injection and using a small number of header droplets. The idea is to insert a header droplet in front of the payload droplet for each module to be skipped. For the realization of such a scheme

[2]$R_D = (\mu_D - \mu)(\alpha L)/(wh^3)$, with L, w and h being the length, width and height of the droplet [10]. The viscosity of the droplet is denoted by μ_D.

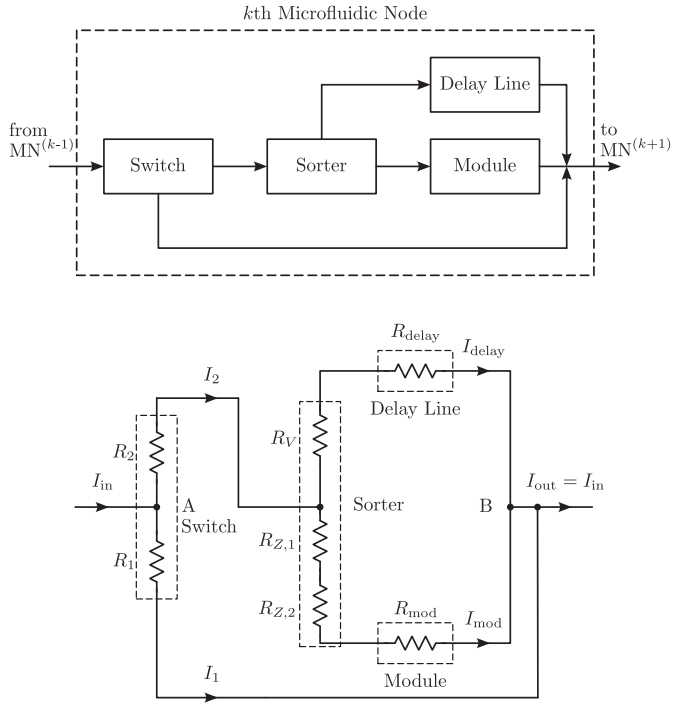

Fig. 3. Proposed microfluidic node and the electrical equivalent circuit (MN$^{(k)}$ denotes the kth microfludic node) .

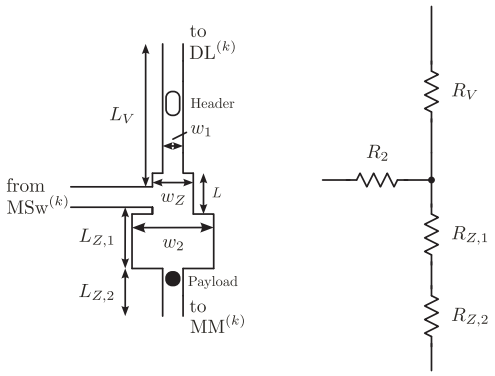

Fig. 4. Droplet by size sorter [12] and the electrical equivalent circuit (MM$^{(k)}$, MSw$^{(k)}$ and DL$^{(k)}$ denote the microfluidic module, the microfluidic switch and the delay line in the kth microfluidic node, respectively.

we exploit the fact that the distance between the payload and the header droplet decreases when traversing through the nodes. If the distance between the payload and the header droplet is sufficiently large, both droplets flow towards the module. If the distance between the payload and the header droplet is below a certain threshold, it must be guaranteed that the payload droplet skips the module. In the former case it must be ensured that only the payload droplet reaches the module, while the header droplet bypasses the module to avoid undesirable reactions. This can be achieved through a droplet by size sorter (cf. Appendix A) placed before the module, assuming that the header and payload droplet size are properly set, as we will describe later. A network node which implements the aforementioned functionality and its electrical equivalent circuit are shown in Fig. 3. The proposed network node represents an extension of the state-of-the-art microfluidic node shown in Fig. 1 by a sorter and a delay line. In the following, we provide a detailed description of the proposed node and how it can be used for addressing multiple nodes.

The switch at the entrance of the node is similar to the switch shown in Fig. 2, but no bypass channel is used. In order to guarantee that a droplet arriving at the T-junction of the switch flows into channel 2 towards the sorter, the following condition must hold:

$$R_1 > R_2 + (R_{\text{delay}} + R_V)||(R_{Z,1} + R_{Z,2} + R_{\text{mod}}). \quad (4)$$

A droplet is forced to enter channel 1 (and flows towards the next node) if a preceding droplet is still in channel 2 and

$$R_1 < R_D + R_2 + (R_{\text{delay}} + R_V)||(R_{Z,1} + R_{Z,2} + R_{\text{mod}}) \quad (5)$$

is satisfied, where R_D denotes the hydrodynamic resistance of the droplet in channel 2. The delay line adjusts the velocity of the droplet by changing the hydrodynamic resistance. The droplet sorter separates the droplets according to its size. We assume that the header droplet size is greater than the payload droplet size and thus the sorter forces the payload and header droplet to flow into the module and the delay line, respectively. We use the passive sorter proposed in [12], whose layout and electrical equivalent circuit is shown in Fig. 4. A brief review on the sorting principle can be found in Appendix A. A prerequisite for the sorter to work properly is

$$(R_{\text{delay}} + R_V) > (R_{Z,1} + R_{Z,2} + R_{\text{mod}}). \quad (6)$$

In order that the payload and the header droplets are sorted appropriately, their size has to be tuned such that the experienced *shear force ratio* (SFR) is below or above 1, respectively (cf. Appendix A). In this way, the header is sorted into the delay line whereas the payload is sorted into the module.

Let's consider a payload and a header droplet with a distance of $D_{\text{HP}}^{(k)}$, which are arriving at the entrance of the kth node, and, thus at the T-junction of the switch. Assuming that (4) is satisfied, the header droplet enters channel 2 and flows through the sorter and the delay line towards the $(k+1)$th node. Depending on the distance $D_{\text{HP}}^{(k)}$, we can distinguish two cases for the payload droplet [7]:

1) *Executing the kth module – $D_{HP}^{(k)} > L_2$:* Since the header droplet has already left channel 2, the payload droplet follows the header droplet into channel 2. It flows through the sorter into the module for processing and afterwards towards the $(k+1)$th node. At the outlet of the kth node the distance between the payload and the header droplet is reduced by D_{exec}, i.e. $D_{\text{HP}}^{(k+1)} = D_{\text{HP}}^{(k)} - D_{\text{exec}}$, with $D_{\text{exec}} < D_{\text{HP}}^{(k)}$.
2) *Skipping the kth module – $D_{HP}^{(k)} < L_2$:* The payload droplet enters channel 1 and flows towards the $(k+1)$th node, since the header droplet is still in channel 2 and (5) is satisfied. In this case it must be ensured that, at the outlet of the kth node, the header droplet is placed behind the payload droplet with a sufficiently large distance so that it does not influence the addressing of the subsequent nodes.

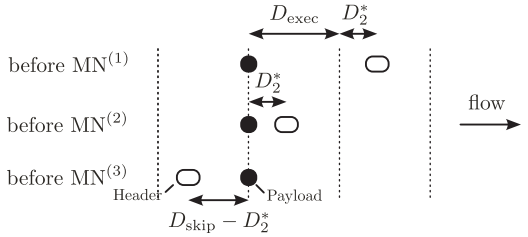

Fig. 5. Droplet sequences when module 1 and 3 are executed and module 2 is skipped (MN$^{(k)}$ denotes the kth microfludic node).

The distance at the outlet of the kth node is reduced by D_{skip}, i.e. $D_{\text{HP}}^{(k+1)} = D_{\text{HP}}^{(k)} - D_{\text{skip}}$, with $D_{\text{skip}} > D_{\text{HP}}^{(k)}$.

The computation of the distance reduction D_{exec} and D_{skip} can be found in Appendix B and depends on the actual realization of the network node. For skipping multiple modules, multiple header droplets are inserted in front of the payload. The distances of the individual header droplets to the payload droplet indicate which module is skipped. The distance at the entrance of the first node that is required to skip the kth module is given by

$$D_{\text{H}_k\text{P}}^{(1)} = k_{\text{skip}} D_{\text{skip}} + k_{\text{exec}} D_{\text{exec}} + D_2^*. \tag{7}$$

The number of modules which are executed and skipped before the kth module are denoted by k_{exec} and k_{skip} ($k_{\text{exec}} + k_{\text{skip}} = (k-1)$) and D_2^* must be smaller than the length of channel 2 of the switch, i.e. $D_2^* < L_2$. Since this scheme requires only an insertion of a header droplet if a module is skipped, it is most suitable when the payload droplet is processed by many modules.

The proposed addressing scheme is now illustrated by means of an example. Consider a ring network with three nodes. The required droplet sequence to skip module 2, i.e. to execute module 1 and 3, is given by a payload droplet and a single header droplet at distance $D_{\text{exec}} + D_2^*$, i.e. $D_{\text{H}_2\text{P}}^{(1)} = D_{\text{exec}} + D_2^*$, with $k_{\text{skip}} = 0$ and $k_{\text{exec}} = 1$. When the payload and the header droplet arrive at the first node, the payload is processed by the module. As the payload and the header droplet traverse through the first node, their distance is reduced by D_{exec}. Thus, the distance between the header and the payload droplet at the entrance of the second node is $D_2^* < L_2$. In this case, the payload skips the module in the second node and the distance between the payload and header droplet is reduced by D_{skip}. After the second node, the header droplet is placed behind the payload droplet at a distance of $D_{\text{skip}} - D_2^*$, since $D_{\text{skip}} > D_2^*$ and, accordingly, will not affect the path followed by the payload anymore. Consequently, the payload is correctly processed in the third node. The droplet sequences at the entrance of the individual nodes are depicted in Fig. 5.

IV. Validation through simulations

We validated the proposed addressing scheme, by evaluating the macroscopic evolution of the droplets path in a ring network with three nodes. To this end, we applied the event-based simulator proposed and thoroughly described in [10], which models the microfluidc network as a time-varying equivalent

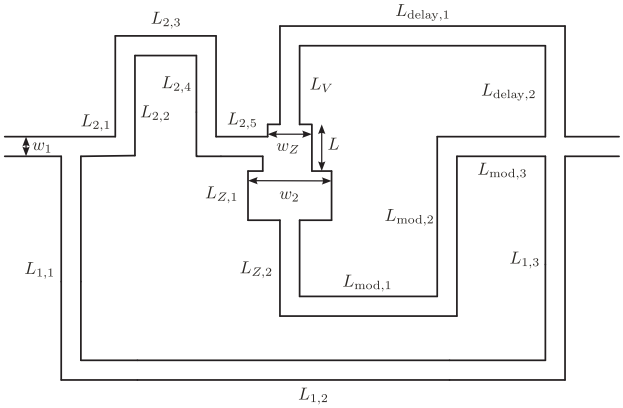

Fig. 6. Layout of the network node used for the simulation. The corresponding channel dimensions are given in Tab. I.

electrical circuit. Note that, since the sorter device was not originally implemented in the simulator, we added this element by associating a vector to the connecting vertex which stores the main parameters of the wide junction of the sorter, i.e. w_2 and L (cf. Fig. 4). If a droplet arrives at the junction, these data are used, together with the size of the droplet and the current flow rates of the channels V and Z, to compute the SFR experienced by the incoming droplet by using (8) – (10). Finally, depending on the result, the simulator determines the path followed by the droplet (channel V if SFR > 1 and channel Z otherwise).

We have designed the network node such that the dimension of the channels are suitable for the actual fabrication of the device and (4) – (6) are satisfied[3]. The layout and the corresponding channel dimensions are provided in Fig. 6 and Tab. I, respectively. According to the network design, the volume of the payload and the header droplet is given by $1.25 \cdot 10^{-5}\,\text{mm}^3$ and $1.625 \cdot 10^{-4}\,\text{mm}^3$, respectively. We chose $D_2^* = 250\,\mu\text{m}$ and applied $Q_{\text{in}} = 10^{-5}\,\text{ml/s}$ as flow rate at the input of the network node. The relation between the resistances in the electrical equivalent circuit in Fig. 3 and the channel lengths in Fig. 6 is given in Tab. II. For example, the resistance R_1 is derived by applying (1) with the channel length $L_1 = \sum_{i=1}^{3} L_{1,i}$, width w_1 and height h. The resistances were used to compute the distance reduction D_{exec} and D_{skip} between the payload and the header droplet, when they traverse through the network node (cf. Appendix B). However, the computation described in Appendix B does not consider the change of the resistance due to the presence of droplets – resulting in approximations for D_{exec} and D_{skip}. We used the approximations as initial values to determine the actual values D_{exec} and D_{skip} through simulations – resulting in $D_{\text{exec}} = 3\,\text{mm}$ and $D_{\text{skip}} = 5.25\,\text{mm}$.

For the validation of our approach we used the example described in the previous section[4]. The payload droplet needs to be processed by module 1 and 3 and, thus, should skip

[3]Typically, R_{mod} is given by the actual realization of the module and the remaining channel lengths and widths are adjusted that (4) – (6) are satisfied.

[4]Please note that we successfully validated other examples which are not covered here due to the lack of space.

TABLE I
CHANNEL DIMENSIONS OF THE NETWORK NODE IN FIG. 6.

Channel lengths $L_{1,1}$, $L_{1,3}$	375 μm
Channel lengths $L_{1,2}$, $L_{V,1}$, $L_{\text{delay},2}$	500 μm
Channel lengths $L_{2,1}$, $L_{2,3}$, $L_{2,5}$	100 μm
Channel lengths $L_{2,2}$, $L_{2,4}$, $L_{Z,2}$	225 μm
Channel lengths $L_{\text{mod},1}$, $L_{\text{mod},3}$	125 μm
Channel length $L_{\text{delay},1}$	200 μm
Channel length $L_{Z,1}$	50 μm
Channel length $L_{\text{mod},2}$	275 μm
Channel length L	75 μm
Channel width w_1	50 μm
Channel width w_2	300 μm
Channel width w_Z	80 μm
Channel height h	50 μm

TABLE II
RELATION BETWEEN THE RESISTANCES AND THE CHANNEL LENGTHS.

Resistance	Channel Length
R_1	$L_1 = \sum_{i=1}^{3} L_{1,i}$
R_2	$L_2 = \sum_{i=1}^{5} L_{2,i}$
R_V	L_V
R_{delay}	$L_{\text{delay}} = \sum_{i=1}^{2} L_{\text{delay},i}$
$R_{Z,1}$	$L_{Z,1}$
$R_{Z,2}$	$L_{Z,2}$
R_{mod}	$L_{\text{mod}} = \sum_{i=1}^{3} L_{\text{mod},i}$

module 2. The required droplet sequence contains a payload droplet and a single header droplet at a distance $D_{\text{exec}} + D_2^*$. We applied this droplet sequence to our network and verified the desired behavior by observing the trajectory of the droplets in the network (cf. Fig. 7).

V. CONCLUSIONS

In this work, we presented a scheme for addressing multiple modules in a microfluidic ring network without complex payload droplet re-injection and the need of a small number of header droplets only. To this end, we have proposed a new network node that allows header droplets to bypass the module and to skip the processing of the payload droplet by the module. For each module that a payload droplet has to skip, a header droplet is inserted in front of the payload at a specific distance. Thus, the proposed scheme enables ring networks to process the payload droplet by different modules with a single injection. We validated our approach through observing the macroscopic evolution of the droplets path in the network. As a future work we will evaluate our approach through experiments.

APPENDIX A
PASSIVE MICROFLUIDIC SORTER

In the following, we briefly describe the principle of the passive sorter proposed in [12]. The layout and its electrical equivalent circuit are shown in Fig. 4. The input channel is connected to a wide junction with the section $w_Z \times L$. The junction is connected to the channel V (width w_1) and the channel Z, consisting of a wide (width w_2) and a narrow channel (width w_1). Since channel Z is shorter than channel V,

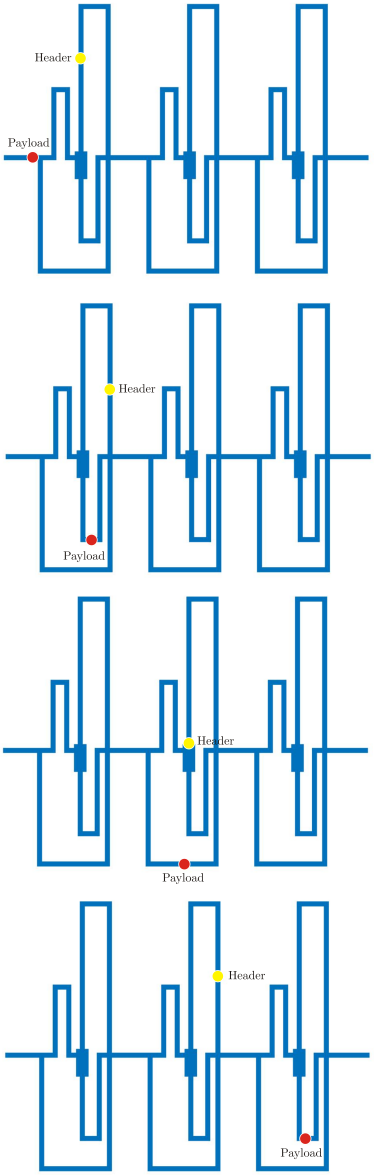

Fig. 7. Screenshots of the droplet evolution in a 3-node ring network, where the payload droplet is processed by module 1 and 3 and skips module 2.

the hydrodynamic resistance R_Z is smaller than R_V. Thus, the flow rate Q_Z is greater than Q_V.

The droplet sorting by size works as follows: Whether a droplet arriving at the junction enters either channel V or Z depends on the shear force it experiences. If the junction is symmetric, i.e. $w_1 = w_2$, all droplets will enter channel Z, since $Q_Z > Q_V$. To compensate this effect, the sorter is designed so that the widths w_2 and w_1 are different. Since the shear rate in the channel is inversely proportional to the square of the channel width, a larger width w_2 would reduce the local shear force exerted by Q_Z on the droplet. At the same time, a narrower width w_1 would increase the magnitude of the local shear force exerted by Q_V on the droplet. The layout of the droplet sorter with $w_2 > w_1$, as depicted in Fig. 4, favors the droplet to flow into channel V, but the higher flow rate Q_Z

pushes the droplet to enter channel Z. The tradeoff between these two effects allows to sort the droplets based on their size. The compound effect of junction geometry and flow rates is accounted in the *shear force ratio* (SFR) between channel V and Z. The SFR is given by[5]

$$SFR = (SRR \times PAR)^{-1} \tag{8}$$

with the *shear rate ratio* (SRR) being

$$SRR \propto \frac{Q_Z}{Q_V}\frac{w_1^2}{w_2^2} \tag{9}$$

and the *projected area ratio* (PAR) being

$$PAR = \frac{r^2\pi - r^2/2(2\theta - \sin(2\theta))}{r^2/2(2\theta - \sin(2\theta))}, \tag{10}$$

where r is the droplet radius at the junction and θ is the central angle. It is important to note the SFR depends on the droplet size through the PAR and, thus, affects the sorting. According to [12] the droplet is sorted into channel V and Z if $SFR > 1$ and $SFR < 1$, respectively. Thus, large droplets enter channel V since the SFR they experience is greater than 1, and, vice versa, small droplets flow into channel Z.

Appendix B
Droplet Delay Computation

In this section, we describe the computation of the delay of the payload and the header droplet when they are flowing through the proposed microfluidic node shown in Fig. 3. By applying the current divider rule to the electrical equivalent circuit shown in Fig. 3, we get[6]

$$I_1 = I_{\text{in}}\frac{R_2 + R_{\text{sort}}}{R_1 + R_2 + R_{\text{sort}}}, \tag{11}$$

$$I_2 = I_{\text{in}}\frac{R_1}{R_1 + R_2 + R_{\text{sort}}}, \tag{12}$$

$$I_{\text{delay}} = I_2\frac{R_{Z,1} + R_{Z,2} + R_{\text{mod}}}{R_{\text{delay}} + R_V + R_{Z,1} + R_{Z,2} + R_{\text{mod}}}, \tag{13}$$

$$I_{\text{mod}} = I_2\frac{R_{\text{delay}} + R_V}{R_{\text{delay}} + R_V + R_{Z,1} + R_{Z,2} + R_{\text{mod}}}, \tag{14}$$

with $R_{\text{sort}} = (R_{\text{delay}} + R_V)||(R_{Z,1} + R_{Z,2} + R_{\text{mod}})$. The resistances are obtained by applying (1) with the corresponding channel dimensions (cf. Tab. I and II). The velocities of the droplets in the channels can be computed by [10]

$$v_x = \frac{Q_x}{w_1 h}, \quad v_{\text{mod},1} = \frac{Q_{\text{mod}}}{w_2 h}, \quad v_{\text{mod},2} = \frac{Q_{\text{mod}}}{w_1 h}, \tag{15}$$

with $x \in \{1, 2, \text{delay}\}$. For example, v_1 denotes the velocity of the droplet in channel 1, which is characterized by the hydrodynamic resistance R_1. The channel widths and the height are given in Tab. I and the flow rates Q can be replaced by the electrical currents I. Using the velocities of the droplets and the corresponding channel lengths (cf. Fig. 6, Tab. I and II) the time it takes for a droplet to flow from point A to B (cf. Fig. 3) can be determined. The time for the header droplet flowing through channel 2 of the switch, the sorter and the delay line can be computed by

$$T_{\text{H}} = \frac{L_2}{v_2} + \frac{L_V + L_{\text{delay}}}{v_{\text{delay}}}. \tag{16}$$

The payload can take two different paths in the network – depending on the distance to the preceding header droplet. In case the payload flows through the channel 2 of the switch, the sorter and the module, the time is given by

$$T_{\text{P,exec}} = \frac{L_2}{v_2} + \frac{L_{Z,1}}{v_{\text{mod},1}} + \frac{L_{Z,2} + L_{\text{mod}}}{v_{\text{mod},2}}. \tag{17}$$

and the delay between the header and the payload droplet can be expressed as

$$D_{\text{exec}} = (T_{\text{H}} - T_{\text{P,exec}})v_{\text{out}}, \tag{18}$$

with $v_{\text{out}} = v_{\text{in}} = Q_{\text{in}}/(w_1 h)$. If the payload flows through channel 1 of the switch, the time is given by

$$T_{\text{P,skip}} = \frac{L_1}{v_1} \tag{19}$$

and the delay between the header and the payload is given by

$$D_{\text{skip}} = (T_{\text{H}} - T_{\text{P,skip}})v_{\text{out}}. \tag{20}$$

[5]It is important to note that, in [12], the shear force ratio is defined by $SFR = SRR \times PAR$. For a symmetric junction, this definition always results in values greater than 1 – indicating that all droplets are sorted into channel V. However, in case of a symmetric junction, it is expected that all droplets flow into channel Z since $Q_Z > Q_V$. Since taking SFR^{-1} reflects this behavior, we suppose that the authors just mixed up channel Z and V.

[6]Note that the following results are approximations, since the change of the resistance due to droplets in the channel is not considered.

References

[1] A. J. Demello, "Control and detection of chemical reactions in microfluidic systems." *Nature*, vol. 442, no. 7101, pp. 394–402, 2006.

[2] D. Mark et al., "Microfluidic lab-on-a-chip platforms: requirements, characteristics and applications," *Chemical Society Reviews*, vol. 39, no. 3, pp. 1153–1182, 2010.

[3] S.-Y. Teh et al., "Droplet microfluidics," *Lab on a Chip*, vol. 8, pp. 198–220, 2008.

[4] M. G. Pollack, A. D. Shenderov, and R. B. Fair, "Electrowetting-based actuation of droplets for integrated microfluidics," *Lab on a Chip*, vol. 2, no. 2, pp. 96–101, 2002.

[5] A. Wixforth, "Acoustically driven planar microfluidics," *Superlattices and Microstructures*, vol. 33, no. 5, pp. 389–396, 2003.

[6] E. De Leo et al., "Networked labs-on-a-chip (NLoC): Introducing networking technologies in microfluidic systems," *Nano Communication Networks*, vol. 3, no. 4, pp. 217–228, 2012.

[7] ——, "Communications and switching in microfluidic systems: Pure hydrodynamic control for networking labs-on-a-chip," *IEEE Trans. Commun.*, vol. 61, no. 11, pp. 4663–4677, Nov. 2013.

[8] A. Biral and A. Zanella, "Introducing purely hydrodynamic networking mechanisms in microfluidic systems," in *Proc. IEEE Int. Conf. Communications*, June 2013, pp. 798–803.

[9] L. Donvito et al., "μ-net: A network for molecular biology applications in microfluidic chips," *IEEE/ACM Trans. Networking*, vol. 24, no. 4, pp. 2525–2538, Aug. 2016.

[10] A. Biral, D. Zordan, and A. Zanella, "Modeling, simulation and experimentation of droplet-based microfluidic networks," *IEEE Trans. Molecular, Biological and Multi-Scale Commun.*, vol. 1, no. 2, pp. 122–134, June 2015.

[11] K. W. Oh et al., "Design of pressure-driven microfluidic networks using electric circuit analogy," *Lab on a Chip*, vol. 12, pp. 515–545, 2012.

[12] Y.-C. Tan, Y. L. Ho, and A. P. Lee, "Microfluidic sorting of droplets by size," *Microfluid Nanofluid*, vol. 4, no. 4, pp. 343–348, 2008.